Total Photoelectric Cross Sections of Copper, Molybdenum, Silver, Tantalum, and Gold at 662 kev†

W. F. Titus*
National Bureau of Standards, Washington, D. C.
(Received February 24, 1959)

The total photoelectric cross sections of copper, molybdenum, silver, tantalum, and gold have been measured at 662 kev. A highly collimated beam of gammas from a Cs-137 source impinged upon a thin disk of a target material. Photoelectrons from a target were detected by a plastic scintillator subtending very nearly 4π steradians. Pulse-height analysis permitted partial resolution of photoelectric and Compton events. After subtraction of unresolved Compton events and correction for coherent scattering effects, the cross sections were found to be 0.125 ± 0.009, 0.700 ± 0.016, 1.198 ± 0.028, 8.55 ± 0.14, and 11.62 ± 0.16 barns, respectively, in satisfactory agreement with theory.

A. INTRODUCTION

THE photoelectric cross sections of copper, molybdenum, silver, tantalum, and gold have been measured at 662 kev. The method of measurement involves the detection in a very nearly 4π geometry of the photoelectrons released from thin foils placed in a highly collimated gamma-ray beam.

The high-energy photoelectric cross section generally is obtained from measurements of total absorption coefficients by subtracting from the total interaction cross section the scattering cross section per atom and, above 1 Mev, the pair production cross section. The scattering cross section includes Compton scattering, with corrections for electron binding effects, and coherent scattering. The dependence of the photoelectric cross section upon atomic number is essentially as Z^5. The energy dependence in the region 500–1000 kev is approximately as $1/E^2$, approaching $1/E$ at still higher energies. At higher energies or intermediate atomic numbers, the photoelectric cross section is a small fraction of the total gamma interaction cross section. For example, for tin at 662 kev, the photoelectric cross section is about 10% of the total cross section. Since neither the correction to Compton scattering for electron binding, nor the coherent scattering cross section, nor the pair production cross section near threshold is well known, the subtraction technique yields photoelectric cross sections of limited accuracy in the high-energy region.

Few direct measurements of the photoelectric cross section at high energy exist. Seeman[1] measured the photoelectric cross section of the K shell in lead at 511 kev with a stated probable error of 3%. Latyshev[2] measured the photoelectric cross section in lead at 2.62 Mev with a probable error of about 30%.

Theoretical calculations of the photoelectric cross section in the K shell have been made by Hulme *et al.*[3] at 0.354 and 1.13 Mev for atomic numbers 26, 50, and 84. Relativistic calculations applicable to the same energy region in the limit $Z/137\ll1$ have been performed by Sauter.[4] Theoretical photoelectric cross sections in the indicated energy region are obtained by interpolation of the results of Hulme *et al.* and Sauter, with corrections for the contributions of the higher shells. A detailed discussion of such an analysis has been published by Grodstein.[5]

B. APPARATUS

The experimental apparatus is illustrated in Fig. 1. A nominally 500 mC Cs^{137} source yielding 662-kev gamma radiation was held on a thin support behind a 12 in. long, $\frac{1}{16}$-in. diameter lead collimator. The radiation leaving the collimator passed through a $\frac{1}{8}$-in. diameter 1-in. thick lead antiscattering aperture and then traversed a $\frac{5}{32}$-in. diameter axial hole in a $1\frac{1}{2}$ in. long, $\frac{5}{8}$-in. diameter plastic scintillator. The plastic scintillator was mounted on a 6 in. long plastic light pipe which in turn was optically coupled to the face of a 5819 photomultiplier tube. The scintillator was rigidly held in position and carefully centered on the gamma-ray beam. A small electromagnet was provided to permit the introduction of a magnetic field perpendicular to the beam direction.

With this arrangement, a small thin target could be placed inside the hole in the scintillator, intercepting the entire gamma-ray beam. Compton and photoelectrons ejected from the target would, with high probability, deposit all of their energy in the scintillator,

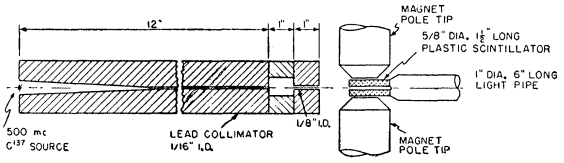

FIG. 1. Schematic of experimental apparatus. See text for description.

† Supported by Office of Naval Research.
* Now at Dartmouth College, Hanover, New Hampshire.
[1] K. W. Seeman, Bull. Am. Phys. Soc. Ser. II, **1**, 198 (1956).
[2] G. D. Latyshev, Revs. Modern Phys. **19**, 132 (1947).
[3] H. R. Hulme *et al.*, Proc. Roy. Soc. (London) **A149**, 131 (1935).
[4] F. Sauter, Ann. Physik **11**, 454 (1931).
[5] G. W. Grodstein, *X-Ray Attenuation Coefficients from 10 kev to 100* Mev (National Bureau of Standards, U. S. Government Printing Office, Washington, D. C., 1957), Circular No. 583.

only a very small fraction, if any, escaping out of the ends of the scintillator. In principle, therefore, the pulse-height distribution from the photomultiplier would exhibit a continuum of smaller pulses due to Compton electrons, with a high-energy cutoff at 478 kev, corresponding to the maximum Compton electron recoil energy from 662-kev gammas. Above the continuum would be a high-energy peak in the vicinity of 662 kev minus the K shell binding energy, due to photoelectrons from the target. The photoelectric cross section would then be obtained simply by measuring the number of photoelectric events per unit time, the target thickness, and the number of gammas incident upon the target per unit time. More simply, the photoelectric cross section could be obtained in terms of the (well known) Compton cross section by comparing the number of photoelectric events from a target with the corresponding number of Compton events. In practice, however, the energy resolution of the system was inadequate to resolve the photoelectric events from the more energetic of the Compton events, and it was necessary to resort to a subtraction technique by measuring the Compton recoil spectrum from a target of low atomic number, in this case aluminum, for which the photoelectric cross section is negligible.

Compton recoil electrons from a thin target all go into the forward hemisphere. At high energies the photoelectron angular distribution is strongly peaked forward. With 660-kev gammas incident, in the Sauter approximation,[4] the angular distribution of photoelectrons peaks in the vicinity of 20°–25° with a strong minimum[6] or zero intensity forward, and fewer than 1% go into the backward hemisphere. In view of this, the targets were placed only $\frac{3}{8}$ in. inside the end of the scintillator nearest the source. In this geometry, the down-beam end of the scintillator hole subtended only 0.12% of the sphere, or a cone of half angle approximately 4°. The up-beam end subtended 1.1% of the sphere, or a cone of half-angle 12°. For the detection of photoelectrons from a target, the scintillator occupied essentially 4π steradians.

High-purity aluminum, copper, molybdenum, silver, tantalum, and gold targets $\frac{1}{8}$ in. in diameter were formed by punching disks from larger sheets of the materials. The punch consisted of a solid steel rod $\frac{1}{8}$ in. in diameter, one end of which was carefully squared off on a lathe to produce a sharp cutting edge. A target disk was punched by placing a sheet of the target material on a piece of firm rubber or Teflon and driving the steel punch through the sheet with a sharp hammer blow. This method has the advantage of simplicity and produces fairly clean edged disks, but has the disadvantage that it may produce nonuniformity in thickness of the disks. The targets were all nominally 10 mg/cm² thick.

Each target was mounted on an approximately 40 μg/cm² thick collodion film which was in turn stretched across one end of a carefully squared $\frac{3}{8}$ in. long, $\frac{5}{32}$-in. o.d. tube made of aluminum foil of nominal thickness 7 mg/cm². Each tube was fitted with a collar at the end opposite the target to facilitate handling and to fix the depth of insertion of the targets into the scintillator. The tubes were a close fit inside the hole in the scintillator, and each target was carefully centered on the axis of its tube; thus, when inserted, the targets were centered on the gamma-ray beam. When the measurements were performed, the targets were 1 in. from the end of the antiscattering aperture, and 3 in. from the end of the beam collimator. In this geometry, the umbral diameter of the beam was $\frac{1}{16}$ in., the over-all diameter $\frac{3}{32}$ in. On the basis of measurements of the beam profile, it is felt that the targets at all times intercepted all of the beam. During the course of the measurements, it was necessary to remount all of the targets several times, due to the fragility of the collodion films. No inconsistencies in the measurements were observed at any time.

Pulses from the photomultiplier were coupled to a cathode follower which then fed both a 256 channel pulse-height analyzer and a linear amplifier. Pulses from the linear amplifier, delay line clipped at one microsecond, were sent to an integral discriminator and scaler for monitoring purposes.

C. MEASUREMENTS

To obtain the photoelectric cross section in the present measurements, three quantities were required. The number per unit time, N_p, of photoelectrons from a target, the target thickness, τ, in the region of the target intercepted by the beam, and the number of 662-kev gammas incident upon the target per unit time, denoted here as the total beam intensity.

1. Measurement of N_P

The photoelectron count from a target was obtained by subtraction from the total pulse height spectrum obtained from a target of background and of unresolved events due to high-energy Compton recoil electrons. The aluminum target served as a pure Compton scatterer for the subtraction. A subtraction depended, with only small corrections, on the ratio of the number of electrons in a target to the number of electrons in the aluminum target. Pulse-height distribution measurements were performed in a cyclic fashion. Pulse-height spectra from two of the higher Z targets and from the aluminum target were measured each for 30 minutes, and background with a collodion film was measured for 10 minutes. A few measurements were made for times as long as 2 hours. Generally a cycle took 2 hours to perform. Four to six cycles were measured in a day. Denoting one day per target as a run, the number of runs per target was copper, 7; molybdenum, 9; silver, 3; tantalum, 4; and gold, 6. Typical pulse-height spectra are illustrated in Fig. 2.

[6] S. Hultberg, Arkiv Fysik **9**, 245 (1955).

The cyclic method of measurement permitted the evaluation of gain drifts, which could affect the subtractions. Relative changes in gain typically were smaller than 0.1% per hour and in all cases introduced negligible error in the subtractions.

The gold runs include one, along with aluminum and background, which was performed with a magnetic field of 3200 gauss perpendicular to the beam and uniform over an area approximately 1 in. in diameter. The fringing field achieved half value at a diameter of approximately 2 in. This measurement was made to test the photoelectron detection efficiency since the magnetic field was of sufficient strength to prevent the photoelectrons from escaping out the hole in the scintillator. After subtraction of background and unresolved Compton events, the photoelectron count per unit time with magnetic field agreed with that without magnetic field to within $\frac{1}{2}$%, with an uncertainty of approximately 1.2%, demonstrating that virtually all of the photoelectrons from the targets were detected in the scintillator.

2. Measurement of Target Thicknesses

The target thicknesses were obtained by weighing the targets on a precision balance, and measuring the target diameters with a traveling microscope. The results of these measurements are summarized in Table I. The first column, τ, gives the target thicknesses measured as described above, the second column, α_w, is the ratio of the number of electrons in each target to the number in the aluminum target, that is, the ratio $(\tau Z/A)_{\text{target}}/(\tau Z/A)_{\text{aluminum target}}$.

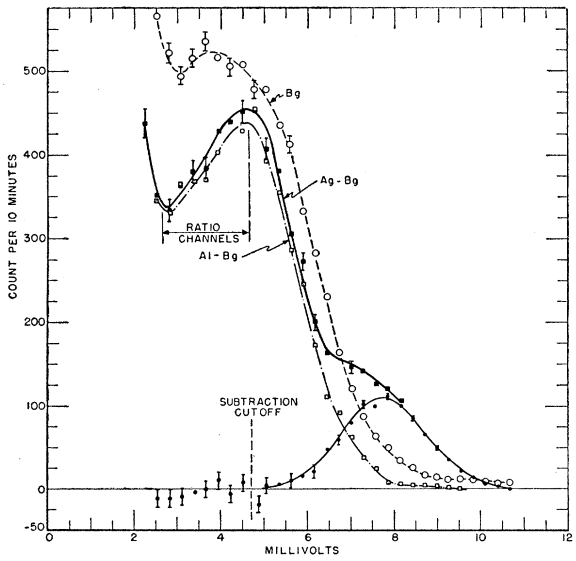

FIG. 2. Typical pulse-height distributions due to silver target, an aluminum target, and background. The distribution peaking at approximately 7.5 millivolts is due to photoelectrons from the silver target and was obtained by subtraction from the silver distribution of the suitably normalized aluminum and background distributions.

TABLE I. See text for explanation of symbols.

Target	τ (mg/cm²)	α_w	α_c'	α_c
Al	9.36±0.8%			
Cu	11.40±0.7%	1.153±1.1%	1.124±0.004	1.124±0.004
Mo	14.56±0.7%	1.412±1.1%	1.340±0.005	1.339±0.005
Ag	10.97±0.7%	1.059±1.1%	1.028±0.006	1.029±0.006
Ta	10.70±0.7%	0.957±1.1%	0.943±0.009	0.947±0.009
Au	12.36±0.7%	1.097±1.1%	1.093±0.010	1.097±0.010

The relative target thicknesses were obtained from the pulse-height distributions as well as from the weighings. The pulse-height region chosen to obtain this ratio is indicated in Fig. 2. This region is below the photoelectron distribution, but above the region where secondary events might be important, especially events due to gammas backscattering from the plastic light pipe into the targets. The rise in the background at low pulse heights, as illustrated in Fig. 2, is believed to be due to gammas which have backscattered from the light pipe. Pulses in the ratio region are due mainly to Compton recoil electrons from the target with energies in the range of 300±100 kev. For recoil electrons of such high energy, the effect of electron binding on the Compton cross section is negligible.[5] Thus, with only small corrections, the ratio of the total number of counts from a target in the ratio region to the corresponding number from the aluminum target is equal to the ratio of the number of electrons in the portion of the high-Z target intercepted by the beam to the number of electrons in the corresponding portion of the aluminum target. The measured ratios are listed in Table I under α_c. The ratios α_c are an average over all of the runs. Individual values were obtained each day a target was measured. The distribution of the values of α_c obtained from day to day for a given target was consistent with the estimated uncertainty.

The column α_c' is α_c corrected for the effects of coherent scattering in the targets. α_c' is to be compared with α_w. Coherent scattering has the effect of increasing the number of observed scintillations at any pulse height. It is negligible for targets of small Z, but becomes significant for targets of high Z. The coherent scattering correction was estimated by calculating the coherent scattering angular distribution[7] for a target and numerically integrating over the thickness of scintillator to be traversed by the scattered gammas, obtaining thereby the total number of scintillations to be expected due to the coherent scattering. In Au, the worst case, the correction was only 0.4%. No correction has been made for the effect of electron binding on Compton scattering. The bound electronic motion has the effect of relaxing the Compton energy-angle relation in the laboratory system and is most important for the atoms of highest atomic number. For bound electrons at rest, a recoil electron will have less

[7] A. T. Nelms and I. Oppenheim, J. Research Natl. Bur. Standards **55**, 53 (1955).

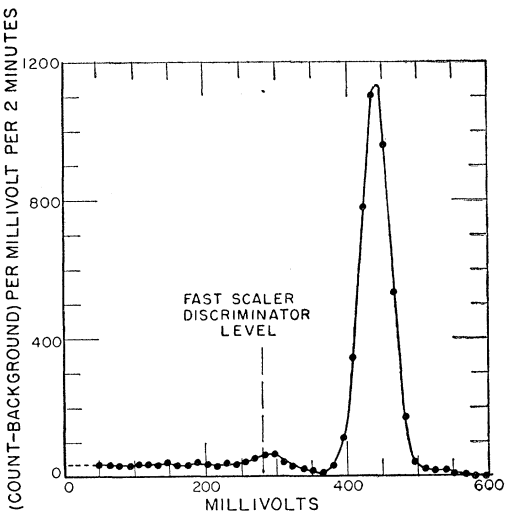

FIG. 3. A typical pulse-height distribution measured with the 4-in. thick by 5-in. diameter NaI(Tl) crystal centered on the gamma-ray beam. This distribution was measured with 33.6 g/cm² lead absorber in the beam. The firing point of the fast scaler discriminator is indicated.

energy than a free electron recoiling into the same direction. In this approximation, it is estimated that only a 0.6% correction would apply to the case of gold, and would act to decrease α_c'. The correction for the targets of lower atomic number would be smaller. The inclusion of the motion of the bound electron will yield a still smaller correction.

3. Beam Measurements

The total gamma-ray beam intensity was measured by means of a 4-in. thick by 5-in. diameter NaI(Tl) crystal. The plastic scintillator and associated equipment were removed from the path of the beam. The heavily shielded NaI crystal was carefully centered with its axis colinear with the beam, at a distance of 41 in. from the end of the collimator, or 38 in. from the point at which the targets were normally held in the beam. The crystal was mounted on a 5-in. diameter Dumont type 6364 photomultiplier tube. The photomultiplier output was coupled to a cathode follower which fed two linear amplifiers. Pulses from the first amplifier, delay line clipped at one microsecond, fed a 10 channel pulse-height analyzer. Pulses from the second amplifier, delay line clipped at one-half microsecond, fed a fast discriminator and scaler. The thickness of the NaI crystal in the path of the beam was 3.91 in.±0.094 in., or, 36.42±0.88 g/cm², taking the density of NaI(Tl) to be 3.667 g/cm³. The front cover of the crystal was aluminum with a reflecting coating of MgO. The total thickness of this cover is stated to be such that the most probable energy loss of 5-Mev electrons traversing it is 300 kev.[8] This loss is equivalent to a thickness of aluminum of 210 mg/cm², which thickness has been assumed here for estimates of absorption. The backing of the crystal, including the photomultiplier tube face was $\frac{5}{16}$-in. glass.

The counting rate with the NaI crystal exposed to the direct beam was too high to permit the use of the 10 channel pulse-height analyzer. Thus, all pulse height distributions were measured with precisely machined lead absorbers interposed in the beam. The absorbers were always placed such that the distance from the down-beam face of the absorbers to the front face of the NaI crystal was 30 in. A typical pulse-height distribution is illustrated in Fig. 3. The firing point of the discriminator in the fast scaler is indicated in the figure.

The beam profile was examined with a 40.27 g/cm² thick lead absorber in the beam. A $\frac{3}{4}$-in. diameter aperture in a 2-in. thick lead block mounted on a milling head was moved across the beam in front of the crystal both vertically and horizontally, and the counting rate from the crystal was measured as a function of the aperture position. The beam profile measured in this way was closely consistent with the profile predicted on the basis of the collimator geometry and the geometry of the scanning aperture.

The absorption coefficient of lead was next measured, using only the counting rate in the fast scaler. In this case, the $\frac{3}{4}$-in. diameter secondary collimator was centered on the beam. The beam diameter at the secondary collimator was 0.46 in. Thus, the secondary collimator intercepted only gammas scattered from the lead absorbers. As a check on consistency absorption coefficient measurements were made with several different thicknesses of lead absorber in place. The absorption coefficient measured in this way is given by the relation below.

$$\mu = (1/\tau)\ln(I_0/I).$$

Here I_0 is the counting rate with no absorber in place, I is the counting rate with an absorber of thick-

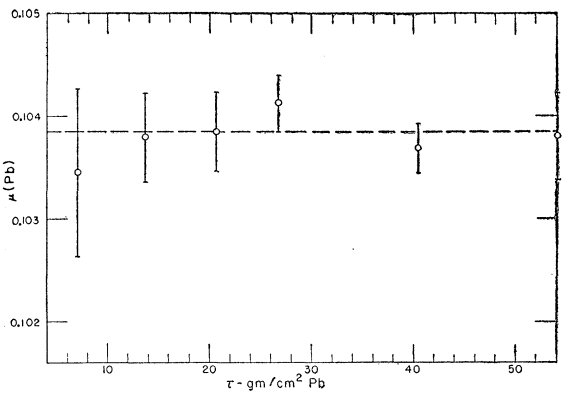

FIG. 4. The absorption coefficient of lead for the 662-kev gamma-ray beam. Measurements were made with thicknesses of lead of 0, 6.9, 13.6, 20.5, 26.7, 40.3, and 53.9 g/cm². In all cases the detector subtended a solid angle of 6.06×10^{-4} steradian at the absorbers.

[8] H. W. Koch (private communication).

ness τ g/cm^2 lead in place. The counting rate losses in the fast scaler were measured at counting rates of 17 000 counts per second (no absorber) and 8500 counts per second (6.9 g/cm^2 lead absorber). This measurement was made essentially by observing the counting rate due to a small secondary Cs^{137} source with and without the main beam incident on the crystal. The results were consistent with a dead time in the system of 2.15 μsec, with an uncertainty of approximately 10%. The results of the absorption measurements are illustrated in Fig. 4. The weighted average of the measurements is $\mu=0.10386\pm0.00014$ cm^2/g lead. This absorption coefficient applies to the measurement geometry in which the secondary collimator subtended a solid angle of 6.06×10^{-4} steradians at the absorbers. This value of the absorption coefficient compares closely with the interpolated value of Colgate[9] of 0.104 for the same secondary collimation geometry.

The photofraction, or ratio of counts in the photo peak to total counts in the pulse-height distribution from the NaI crystal was measured with lead absorbers of thicknesses 33.61, 40.27, and 47.19 g/cm^2 in the beam. The average uncorrected photofraction measured in this way was 0.811 ± 0.002. When correction is made by means of a single scattering calculation for scattered radiation from the front cover of the crystal and from the glass backing behind the crystal, a final value of 0.821 ± 0.003 is obtained, in very close agreement with the value of 0.821 ± 0.004 of Berger and Doggett[10] obtained by a Monte Carlo calculation for a NaI(Tl) crystal of the same dimensions.

The total beam intensity at the crystal is based on the pulse-height distribution measurements with 40.27 g/cm^2 lead absorber, and upon the average value of the absorption coefficient of lead measured with the fast scaler. The total beam intensity at the plastic scintillator, taking into account the NaI crystal thickness, events in the front and back covers of the NaI crystal, and air absorption, is calculated to be 22 090 662-kev gammas per second with an uncertainty of 0.8%. On the basis of the absorption coefficient and photofraction measurements, contamination of the beam by degraded radiation of energy at all comparable to 662 kev is believed to be negligible.

D. RESULTS

In order to obtain the photoelectron count from each target, it was necessary to subtract the contributions of background and of unresolved high-energy Compton recoil electrons. This subtraction can be written in the form

$$N_p=T-\alpha\mathrm{Al}+(\alpha-1)B_g,$$

where N_p is the photoelectron count, T is the target count, Al is the aluminum target count, and B_g is the background. All counts are total counts per unit time above a fixed threshold level. The fixed threshold level was selected to be below the pulse-height distribution due to photoelectrons. The relative position of the fixed threshold level for the silver subtraction is indicated in Fig. 2. The quantity α is the ratio of the number of electrons in the target to the number of electrons in the aluminum target. Corrections were made for the effects of coherent scattering from the targets and of photoelectrons from the aluminum target. α was measured in two ways as described in section C-2. The results of these measurements are listed in Table I as α_w and α_c', respectively. Comparison indicates a considerable discrepancy in several cases. In an attempt to resolve this discrepancy, the targets were examined for thickness nonuniformities. Each target was mounted on an approximately 50 μg/cm^2 thick collodion film on a ring support. A target was then moved across a 0.020-in. diameter collimated beam of copper $K\alpha$ x-rays in an x-ray diffraction unit, and the transmitted intensity of the x-rays was measured as a function of the target position. The absorption of the aluminum and copper targets was too small to permit the detection of thickness variations smaller than appproximately 4% with certainty. In all of the other foils, thickness variations of the order of 1% were dependably detectable. All of the foils exhibited thickness variations ranging from approximately 1% in silver to 6% in tantalum. Although these measurements were not quantitative in the sense of determining the average thickness of each foil traversed by the beam, they do indicate that the discrepancies between α_w and α_c' exhibited in Table I may be due to thickness variations of the foils. If, in particular, the region of the aluminum foil traversed by the beam is approximately 2.6% thicker than the weight/area measurement indicates, then satisfactory agreement between α_w and α_c' would be obtained. It is felt that an effect of this kind is most probable, and that the values α_c' are the best measures of the relative thickness of the foils traversed by the beam. Quantitative analysis of the aluminum, molybdenum, and silver foils indicates the presence of no contaminant in sufficient quantity to affect the measurements.

In view of the discrepancy between α_w and α_c', the photoelectric cross section has been calculated by three methods. The basic equation for the cross section is

$$\sigma_p=N_pA/N_0\tau L,$$

where N_0 is the number of beam gammas incident upon the target per unit time, N_p is the number of photoelectrons emitted per unit time, A is the atomic weight of the target material, τ is the target thickness in g/cm^2, and L is Avogadro's number. The results of the calculations are tabulated in Table II and plotted in Fig. 5 along with theoretical values interpolated from Grodstein.[5]

[9] S. A. Colgate, Phys. Rev. **87**, 592 (1952).
[10] M. J. Berger and J. Doggett, J. Research Natl. Bur. Standards **56**, 355 (1956).

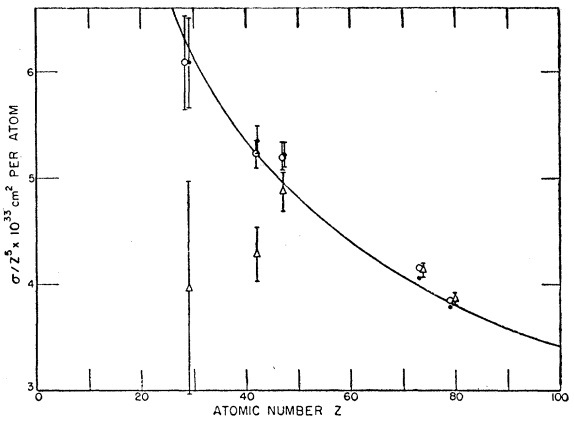

FIG. 5. The photoelectric cross section $\sigma Z^{-5} \times 10^{33}$ cm^2 per atom at 662 kev *versus* atomic number, Z. The points represent the experimental results obtained by the three methods of calculation: closed circles, method A; open circles, method B; triangles, method C. See text for description of the methods of calculation. The indicated uncertainties include all known sources of error. The smooth curve represents the theoretical prediction and was interpolated from Grodstein.[5]

Method A: The subtraction was based upon the ratios α_c'. It was assumed that the effective thickness of the aluminum target was 2.6% greater than was indicated by the weight/area measurement. The cross sections were calculated using target thicknesses obtained from the ratios α_c' and the assumed thickness of the aluminum foil.

Method B: As in method A, the subtraction was based upon the ratios α_c' but the cross sections were calculated using the target thicknesses in column 1 of Table I.

Method C: The subtraction was based upon the ratios α_w and the cross section was calculated using the target thicknesses in column I of Table I.

Uncertainties in the cross sections were calculated in a fashion consistent with the assumptions in each method and included all known sources of error.

At high Z the cross section is practically independent of the method of calculation whereas at low Z, in method C, the cross section is drastically changed. This effect is due mainly to the fact that the subtraction is favorable at high Z whereas at low Z the subtraction involves a small difference between two large quantities.

In view of the consistency of the measured values α_c and the observed thickness variations in the foils, it is believed that the cross sections obtained by method A are the most dependable. In this case the cross sections appear to be slightly larger than the theoretical cross section in the region of intermediate atomic number. The differences, however, are not far outside the experimental error, nor in serious disagreement with the theoretical results which are accurate to not better than ±4%.

TABLE II. Total photoelectric cross section per atom, in units of 10^{-24} cm^2.

	Method A	Method B	Method C	Theoretical interpolated from Grodstein[a]
Cu	0.125±6.9%	0.125±7.0%	0.081±25.4%	0.128
Mo	0.700±2.3%	0.683±2.4%	0.560± 5.8%	0.685
Ag	1.198±2.3%	1.194±2.4%	1.116± 3.6%	1.14
Ta	8.55 ±1.6%	8.63 ±1.4%	8.57 ± 1.5%	8.28
Au	11.62 ±1.4%	11.85 ±1.3%	11.88 ± 1.3%	11.8

[a] See reference 5.

ACKNOWLEDGMENTS

The author wishes to thank Ugo Fano, Evans Hayward, and John Hubbell for many stimulating discussions and helpful suggestions.